

## Evaluation of the mechanism of gelation of an oleogel based on a triterpene extract from the outer bark of birch

M. GRYSKO, R. DANIELS

Received November 26, 2012, accepted December 11, 2012

Prof. Dr. Rolf Daniels, Pharmazeutische Technologie, Eberhard Karls Universität Tübingen, Auf der Morgenstelle 8, 72076 Tübingen, Germany  
 rolf.daniels@uni-tuebingen.de

Dedicated to Prof. Dr. Theo Dingermann, Frankfurt, on the occasion of his 65th birthday.

Pharmazie 68: 572–577 (2013)

doi: 10.1691/ph.2013.6515

Oleogels are known for their high physical, chemical, and mechanical stability and good *in vivo* efficacy, which make them appropriate vehicles for dermal drug delivery and skin care for very dry skin. Modern formulation research focusses on well tolerated and sustainable formulation concepts. This paper deals with an innovative oleogel, which is based on a triterpene dry extract from the outer bark of birch (TE). In this formulation TE does not only act as an excipient but provides interesting pharmacological properties at the same time. The oleogel was formulated using solely *Simmondsia Chinensis* seed oil (jojoba oil) and TE. Fluorescence microscopy and confocal Raman microscopy showed that suspended TE particles arrange in a three-dimensional gel network. Infrared spectroscopy revealed that the formation of hydrogen bonds between TE particles is responsible for the self-assembly of TE in oil. Moreover, the influence of TE concentration and morphology of the TE particles on the viscoelasticity of the resulting oleogels was analyzed. Gel strength increased with TE concentration and was critical to the specific surface area of the TE particles.

### 1. Introduction

Triterpenes are biologically active secondary plant metabolites. Their various pharmacological properties like anti-inflammatory, anti-viral, and wound healing effects are well investigated and specified in the literature (Altinier et al. 2007; Moura-Letts 2006; Pavlova et al. 2003). Even in cancer treatment triterpenes are known as potent agents (Laszczyk 2009). These substances are widely distributed in plants but only the outer bark of the white barked birches contains up to 34 % (w/w) betulin, a pentacyclic triterpene (Ekman 1983). A well characterised triterpene dry extract from the outer bark of birch (TE) contains about 80 % (w/w) betulin, a lupan type triterpene with two polar hydroxyl groups, located on opposite sides of the molecule (Fig. 1).

TE is obtained by accelerated solvent extraction with n-heptane (Jäger et al. 2008). Further identified main constituents of the dry extract are lupeol (LU), erythrodiol (ER), betulinic acid (BA) and oleanolic acid (OA) (Laszczyk et al. 2006). However, the poor solubility of these triterpenes in polar and non-polar solvents (Jäger et al. 2007; Laszczyk et al. 2006) has limited a broader therapeutic application. Only 0.28% (w/w) of the TE are soluble in jojoba oil and <0.0001% (w/w) are soluble in water (Jäger et al. 2008). In order to make use of the therapeutic potential of the TE, it has been found by chance that TE forms spreadable thixotropic gels when suspended in lipids, which can absorb up to 60 % water yielding a stable w/o emulsion (Laszczyk et al. 2006). Obviously, TE does act as an active and an excipient at the same time. This finding fits well with recent demands for well tolerated and more environmentally

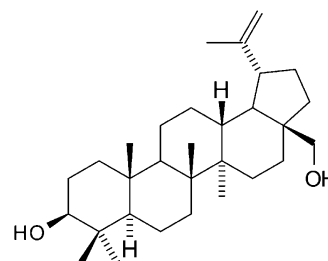


Fig. 1: Chemical structure of betulin.

acceptable semisolid formulations in the pharmaceutical, cosmetic and food industries (Balasubramanian et al. 2012; Sánchez et al. 2011). Furthermore, the use of oleogel based products is increasing, which may be attributed to their long-term stability (Murdan 2005).

The investigated oleogels are stable, semisolid formulations which consist solely of *Simmondsia Chinensis* seed oil (jojoba oil) and TE. The aim of this study was to clarify the factors which are responsible for the gelling properties of a TE.

### 2. Investigations and results

The gel character of differently concentrated TE suspensions was analyzed by measuring the storage modulus ( $G'$ ) and the loss modulus ( $G''$ ) while the material was subjected to an increasing oscillating shear strain (amplitude sweep) (Fig. 2). At low deformation  $G'$  and  $G''$  are constant and the linear viscoelastic (LVE) range is reached, where the sample structure

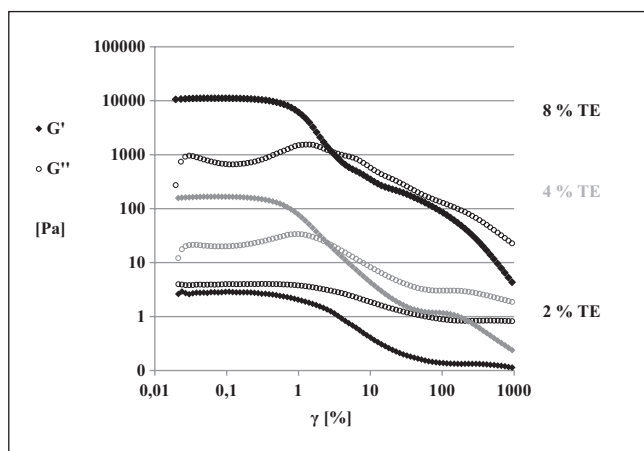


Fig. 2: Amplitude sweeps of TE suspension in jojoba oil with different TE concentrations. Concentration is given as % (w/w)

is undisturbed. The gel character of a system is displayed by a storage modulus  $G'$  exceeding the loss modulus  $G''$ . In this case the sample behaves more like a viscoelastic solid. Consequently the  $G'$ -value in the LVE region is used as parameter for the gel strength.

TE suspensions exhibit viscoelastic behavior when the TE concentration exceeds 2%. The gel strength increases with increasing TE concentration while the loss factor  $\tan \delta$  ( $G''/G'$ ) and the yield stress as determined from the crossover ( $G'' = G'$ ) remain almost constant.

Swelling tests of TE in jojoba oil revealed a volume increase of only  $83 \pm 5\%$ . Accordingly only a minor amount of the oil phase is immobilized by swelling and could therefore not account for the gel formation.

The spatial distribution of the TE particles in a 6% (w/w) suspension in jojoba oil can be seen from fluorescence and confocal Raman micrographs. Figure 3 shows an irregular wide-meshed network structure of agglomerated TE particles.

Due to the chemical structure of betulin, the main constituent of the TE, particle-particle interactions in unpolar media via hydrogen bonds are likely. Infrared spectroscopy was used to investigate the TE suspensions for the occurrence of such interactions (Geisseler and Seidel 1977; Günzler and Gremlich

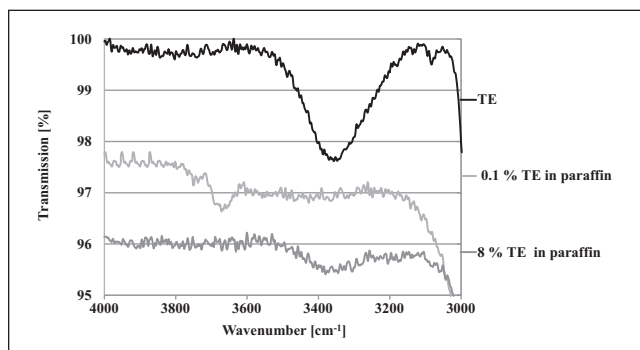


Fig. 4: FTIR spectra of TE 8% (w/w) in paraffin, showing the hydrogen bonds between wavenumbers  $3500$  to  $3300\text{ cm}^{-1}$

2003). Figure 4 shows FTIR spectra of TE powder, and suspensions with 0.1%, and 8% (w/w) TE in paraffin, respectively. Paraffin was used in these experiments instead of jojoba oil because it is not able to form hydrogen bonds by itself. It is thus better suited to determine hydrogen bonds within the gel. As there is almost no interaction between paraffin and TE, higher amounts of TE are required to form a weak gel. Therefore these experiments were done with 8% suspensions of TE in paraffin. TE powder shows a broad peak between  $3500\text{ cm}^{-1}$  and  $3100\text{ cm}^{-1}$ . The peak between  $3700\text{ cm}^{-1}$  and  $3600\text{ cm}^{-1}$  visible with 0.1% (w/w) TE in paraffin, can be assigned to OH-vibration of free hydroxyl groups (Günzler and Gremlich 2003). At a concentration of 8% (w/w), TE particles interact with each other and form an oleogel. This is accompanied by a large shift and a significant broadening in the OH-region (from  $3500\text{ cm}^{-1}$  to  $3300\text{ cm}^{-1}$ ) and can be assigned to hydrogen bonds between superficial hydroxyl and carboxyl groups.

TE partially loses its ability of gelation after thermal stress ( $120\text{ }^\circ\text{C}$ , 2 h). This was confirmed by subjecting oleogels made from tempered TE to oscillatory rheological measurements (Fig. 5).

Suspensions from tempered TE (6% (w/w)) in jojoba oil still show visco-elastic properties with  $G' > G''$ . However, the gel strength dramatically decreased ( $G'_{\text{tempered}} = 54\text{ Pa}$ ) when compared to oleogels made of untreated TE ( $G' = 412\text{ Pa}$ ).

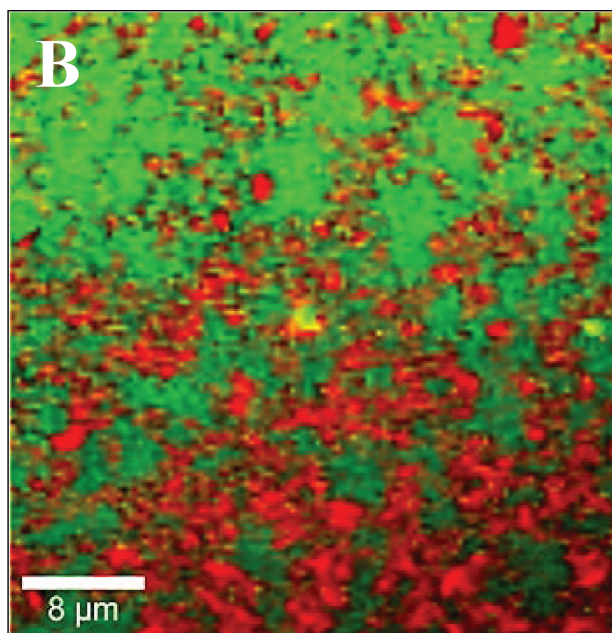
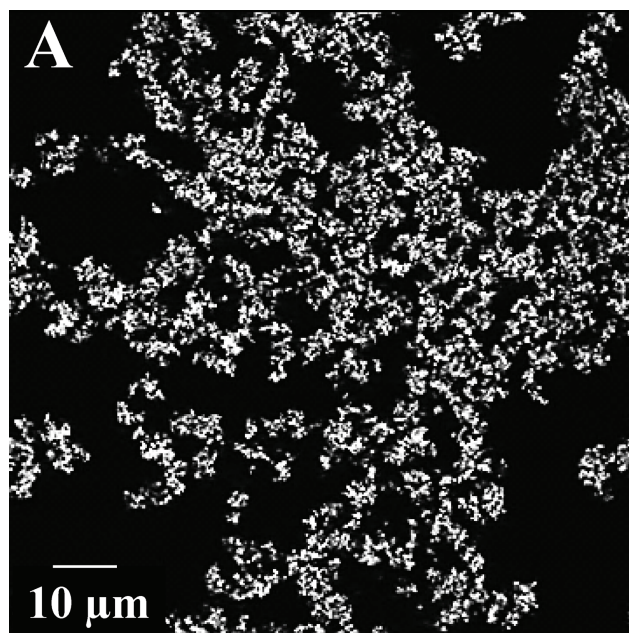


Fig. 3: Fluorescence micrograph of TE 6% (w/w) in jojoba oil (A); Color-coded Raman picture of TE 6% (w/w) in jojoba oil (B): red = TE; green = jojoba oil

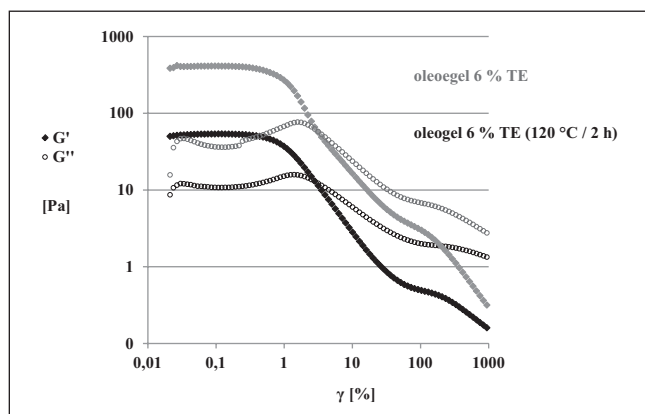


Fig. 5: Amplitude sweep of oleogel containing 6% (w/w) TE before and tempering (120 °C for 2 h)

Concurrently, thermal treatment changes the morphology of the TE and its specific surface area. Untreated TE is characterized by a fragile, porous surface structure (Fig. 6A) with a high specific surface area of  $42 \pm 0.4 \text{ m}^2/\text{g}$ , whereas tempered TE (2 h/120 °C) has a smooth and thready surface (Fig. 6B) combined with a reduced specific surface area of  $21 \pm 0.5 \text{ m}^2/\text{g}$ . DSC measurements allow to follow potential energy changes due to phase transition or decomposition processes during the thermal treatment of the TE. Figure 7 shows representative thermograms of the TE and its two main constituents, betulin and lupeol as a reference. The characteristic melting peak of betulin at 259 °C indicates a pure, crystalline substance. Lupeol shows two endothermic processes at 152 °C and 210 °C, suggesting the existence of two modifications. The initial part of the heating curve of the TE displays the melting of a metastable modification. The subsequent exothermic process specifies the recrystallization to a more stable form, which then melts at 249 °C, indicating the existence of a complex crystalline system. Expectedly, the melting behavior of the stable form is largely affected by betulin and lupeol, the main components of TE. After thermal treatment, the thermogram of the TE remained unchanged (Fig. 8).

X-ray powder diffractograms (Fig. 9) confirm an unchanged crystal structure of TE after heat treatment. Both diffractograms of untreated and tempered TE, respectively, show identical reflexes with slightly decreased peak intensity for the tempered sample.

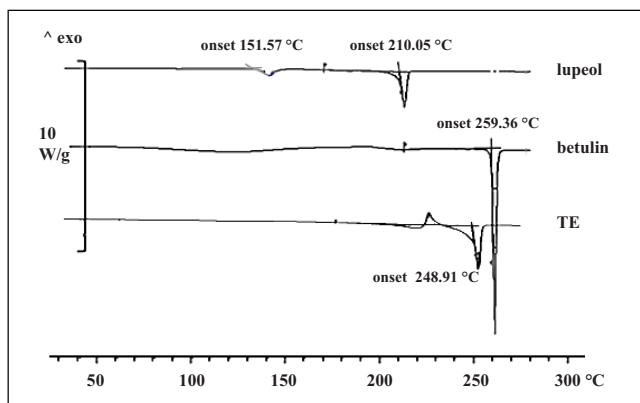


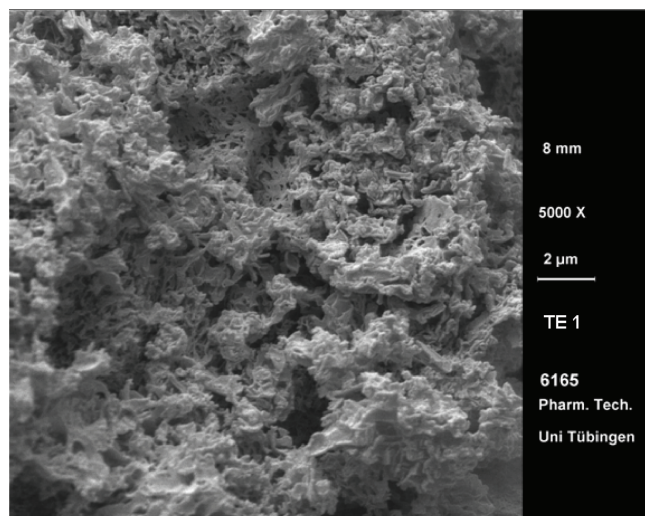
Fig. 7: DSC thermogram of betulin standard, lupeol standard and TE

To specify the influence of the surface area of the TE particles for the gelation, a different birch cork extract (TE-raw) containing 89% betulin (w/w), which shows no gel formation in oil, was recrystallized using accelerated solvent extraction (ASE). The specific surface area was measured and SEM micrographs were taken before and after the recrystallization (Fig. 10). The differences between the surface structures before and after the recrystallization can be seen very clearly. While the original extract shows elongated, fibrous particles and edged surface structures, the surface became fine and porous after the recrystallization. As expected the specific surface area increased drastically during recrystallization from  $3.32 \pm 0.04 \text{ m}^2/\text{g}$  to  $29.0 \pm 0.2 \text{ m}^2/\text{g}$ . Moreover, the recrystallized extract forms a gel when suspended in oil, whereas the original TE-raw was not able gel even at high concentrations.

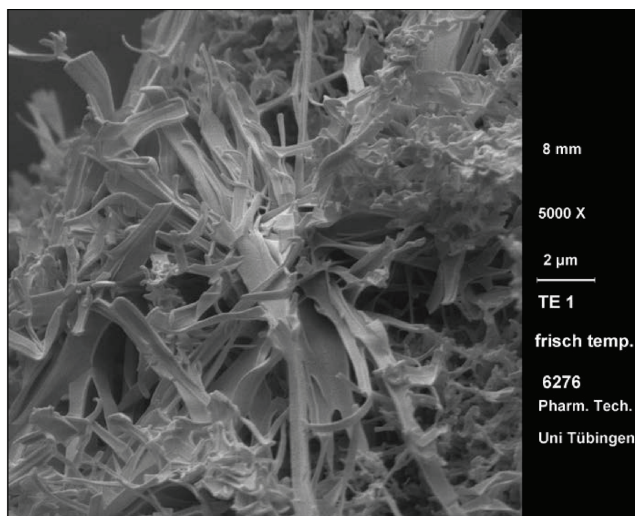
### 3. Discussion

An oleogel is a semi-solid, visco-elastic material composed of a liquid organic phase entrapped in a three-dimensional network. The solubility and particle dimensions of the structurant are important characteristics for the rheological properties and firmness of the oleogel.

Gelling agents for oleogels belong to very different classes, e.g. surfactants, polymers, and solids. Surfactants form well-ordered lyotropic mesophases which immobilize the oily liquid. Polymers usually swell in the oil and form physically bonded, predominantly disordered polymer networks.



(A)



(B)

Fig. 6: SEM photographs of TE (A): before stressing (B): after 2 h stress at 120 °C

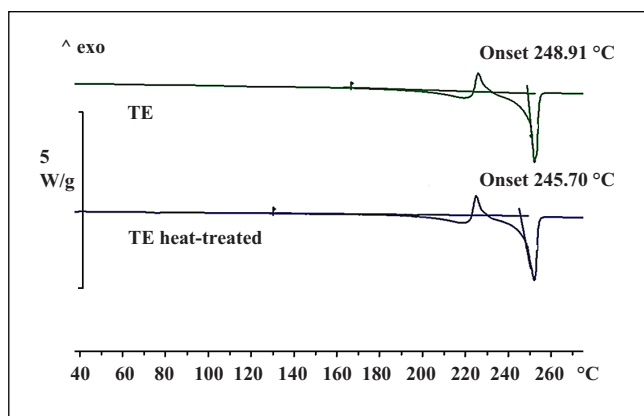


Fig. 8: DSC thermogram of TE before and after 2 h stress at 120 °C

Interactions between polymers can be by due to simple entanglement, H-bonding, or ionotropic crosslinking leading to partially ordered loci. Solid gelling agents immobilize oils usually by the formation of a solid gel network where the solid particles aggregate via ionic interactions or hydrogen bonds.

TE is only marginally soluble in oils and shows only a 1.8-fold volume increase upon swelling. Fluorescence and confocal Raman micrographs show a loose network structure of aggregated TE particles. Such a three-dimensional particulate network is comparable to that described for colloidal silica particles (Bombar and Horsch 1977; Kutz et al. 2011). The resulting oleogels are weak physical gels with a flow stress of 5 Pa as determined from the cross-over of oscillation measurements. Interestingly the flow stress does not vary substantially with increasing TE concentration in the gel. Obviously the interacting forces between the particles are homogeneous and remain the same even when the number of interacting particles increase and form a denser network with a higher consistency at rest. This might be due to the type of interaction between the particles which is frequently hydrogen bonding (Dassanayake et al. 2011; Laredo et al. 2011). This hypothesis is supported by the FTIR measurements which clearly show that TE particles interact by hydrogen bonds between superficial hydroxyl and carboxyl groups. However below 2 % TE gel formation is not possible because the particle density is too low to allow the formation a continuous three-dimensional network of the aggregated particles.

Thermal treatment of the TE demonstrated impressively the importance of the particle morphology of the gelling agent for the rheological properties and firmness of an oleogel. Storing the TE for 2 h at 120 °C decreased substantially its specific surface

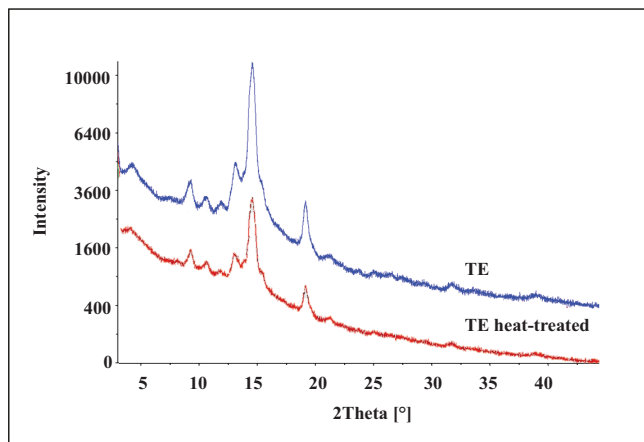


Fig. 9: X-ray diffractograms of TE and crystalline botulin

area and impaired its ability to form gels. This phenomenon has been observed earlier and sintering processes have been hypothesized as a possible reason (Laszczyk 2007). Although the morphological changes can be clearly seen from SEM pictures and BET measurements, the surface transformations could not be retrieved by thermo-analytical techniques (DSC, TG) and x-ray diffraction. This transformation is apparently a matter of a process, which causes only minor changes in the enthalpy of the system and happens without mechanical forces and below the melting temperature of the TE. Particles with a high specific surface area have a high free energy. Thus, for entering a more stable state, the free energy of the system must be decreased (Henrich et al. 2007). This process can be described by (Tramosljika, 2007):

$$\Delta G_T = \Delta G_V + \Delta G_{KG} + \Delta G_S$$

with  $\Delta G_T$  as the total free energy of the system [J],  $\Delta G_V$  as free volume energy [J],  $\Delta G_{KG}$  particle size energy [J] and  $\Delta G_S$  as free surface energy [J].

With a decreasing surface area, the free total energy of the system is reduced. In the case of sintering, the heat effects a compaction of the powder without passing the state of melting (Schatt 1992). This leads to thermal active solid reactions, primarily controlled by diffusion processes. As a result the morphology and the specific surface area are altered but the crystalline state is maintained.

Consequently, the loss in gelation power has to be attributed to the decrease in specific surface area and not to changes in the solid state characteristics of the TE.

An explanation for the observed decrease of gelation due to the sintering process is depicted schematically in Fig. 11. It was shown that gelation is caused by hydrogen bonds between the superficial hydroxyl groups of TE particles. Before the sintering, the fragile particles could be fragmented to smaller pieces which still have a sufficiently high number of superficial OH- and COOH-groups. Upon the sintering process, compact particles are formed, which have a clearly reduced number of superficial functional groups even after grinding them during gel preparation.

Consequently, the opposite effect was observed when TE-raw which has a low specific surface area was subjected to ASE process which increased the surface by a kinetically controlled crystallization process.

In conclusion, the mechanism of the oleogel formation with TE is based on hydrogen bonds between hydroxyl and carboxyl groups at the surface of the TE particles. The ability for gel formation increases with the specific surface area of the TE which can be achieved by a rapid crystallization from solution like it is possible with the ASE process.

## 4. Experimental

### 4.1. Materials

Triterpene dry extract (TE) from the outer bark of birch (Birken AG, D-Öschelbronn), jojoba oil (Gustav Hees, D-Stuttgart), triterpene standards betulin 95,2% (MP Biomedicals, F-Ilkirch), lupeol >95% (Sigma-Aldrich Chemie GmbH, D-Steinheim), TE-raw (89% betulin, GUP "CNLHI", RU-Nischni Nowgorod).

### 4.2. Preparation of oleogel and emulsions

TE was sieved (sieve size 500  $\mu\text{m}$ ) and dispersed in jojoba oil using an Ultra-Turrax® T 25 (IKA, D-Staufen) at 3400 rpm for 2 min. After intermediate cooling for 4 min, homogenization was repeated at 8000 rpm for another 2 min.

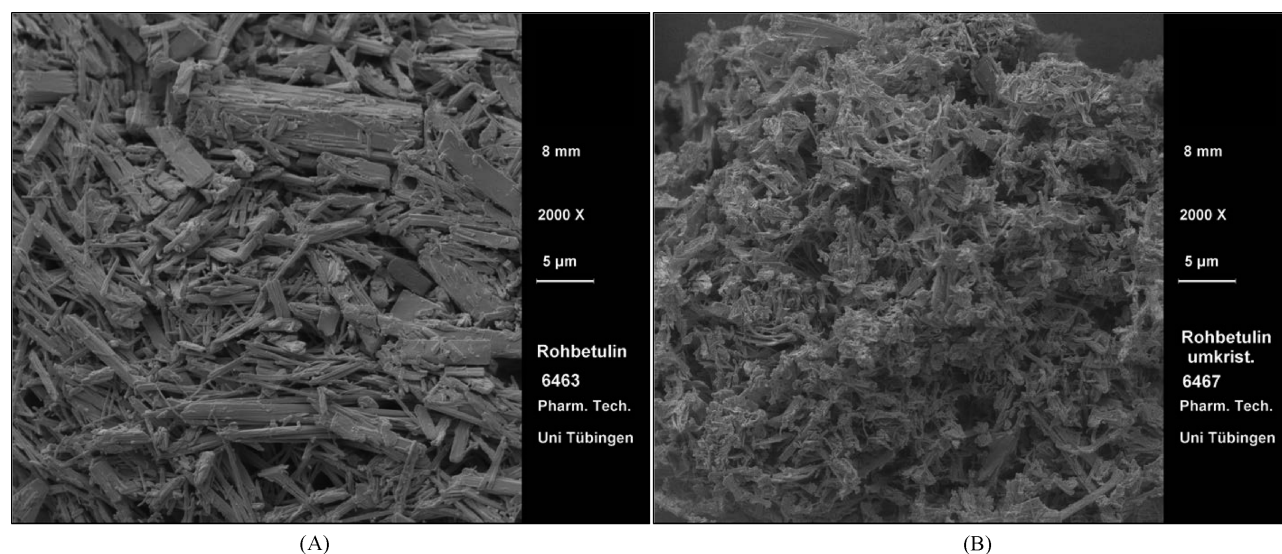


Fig. 10: SEM micrographs of TE-raw before (A) and after (B) recrystallization using ASE.

#### 4.3. Confocal Raman microscopy

Confocal Raman images were taken with a Raman microscope Alpha 500R (WITec, D-Ulm) using a 532 nm excitation laser. The scans were carried out with a 40x objective. The scan range was 30  $\mu\text{m}$  x 30  $\mu\text{m}$ , at 120 x 120 pixels and an integration time of 0.1 s.

#### 4.4. Fluorescence microscopy

The fluorescence micrographs were taken with the Axio Imager Z1 (Carl Zeiss, D-Jena) using the filter set 38 HE eGFP with an excitation range of 470/40 nm. The resulting emission range was 525/50 nm.

#### 4.5. Swelling behavior

At first, 1 g of TE was compacted in a 50 mL disposable syringe (Braun, D-Melsungen) to a yield a bulk volume of 5 mL. Subsequently, the TE was carefully layered with 100 mL oil without disturbing the planar surface at the top of the compacted bed. After 48 h, the volume of the swollen TE was determined.

#### 4.6. Fourier-transform infrared spectroscopy (FTIR)

Infrared spectra were obtained using a FTIR spectrometer Spectrum One (Perkin Elmer, D-Rodgau) equipped with an attenuated total reflectance unit with a diamond crystal. Solid and liquid samples were spread thinly on the surface of the optical waveguide and measured without pressure. Spectra were recorded in the wavenumber range from 4000–670  $\text{cm}^{-1}$ .

#### 4.7. Rheology

Rheological investigations were done at a temperature of 23 °C using a Physica MCR 501 rheometer (Anton Paar, D-Ostfildern). Amplitude sweeps were performed using the parameters listed in the Table.

#### 4.8. Accelerated solvent extraction

TE was recrystallized using accelerated solvent extraction (ASE 300, DIONEX, D-Idstein). The extraction cell was filled with TE-raw and inserted

into the oven. Subsequently, the extraction cell was flooded with n-heptane, set under pressure (100 bar) and heated up to 120 °C. Pressure and temperature were kept constant for 5 min. After the extraction process, fresh solvent for washing was added. The solution was partially discharged at excess pressure through a filter into the collecting vessel. This extraction cycle was repeated twice. At the end of the extraction process, the hot solution was discharged through a filter into the collecting vessel where crystallization took place. The crystallized particles were filtered and dried for 2 h at 80 °C.

#### 4.9. Specific surface area

The specific surface area was determined by gas-adsorption method using a Coulter SA3100 (Coulter Electronics GmbH, D-Krefeld). TE (1–1.5 g) was outgassed for 4 h at 40 °C. Measurements were performed using the static dosing method. The data were treated according to the Brunauer, Emmett and Teller (BET) adsorption isotherm equation (Brunauer et al. 1938).

#### 4.10. Differential scanning calorimetry (DSC)

DSC thermograms were obtained using a TA-8000 (Mettler Toledo, D-Giesen) under a nitrogen gas flow of 10 mL/min. Temperature calibration of the DSC instrument was carried out using indium as a standard. TE (1–3 mg) was analyzed in perforated aluminum standard crucibles at a heating and cooling rate of 10 K/min from 30 °C to 280 °C. Cooling was accomplished with a liquid-nitrogen cooling-accessory.

#### 4.11. Wide angle X-ray powder diffraction (WAXD)

WAXD was performed using a diffractometer PW 3040/60 (Philips, D-Kassel) with a PW 3373/00 tube (copper anode), a tube voltage of 45 kV and an anode current of 40 mA. The size of the fixed divergence aperture is 0.25°. All measurements were carried out at a temperature of 25 °C.

Acknowledgements: The authors thank S. Jäger and K. Hoppe (Birken AG) for carrying out the Accelerated Solvent Extractions and Dr. S. Reichl and Dr. M. Harms (TU Braunschweig) for performing the X-ray measurements.

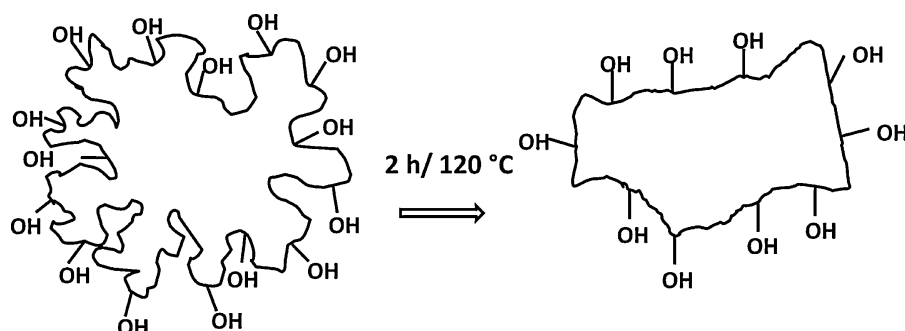


Fig. 11: Schematic diagram showing the surface transformation during TE stress (120 °C/2 h)

**Table: Parameters used for amplitude sweeps**

	pre shearing (rotation)	resting period	amplitude sweep
Shear rate $\gamma$ [1/s]	5		
Deformation $\gamma$ [%]			Start: 0,1 end: 1000 (log. ramp)
Angular frequency $\omega$ [1/s]			1
Number of measuring points	2	1	100
Measuring point duration [s]	20	300	2

**References**

- Altinier G, Sosa S, Aquino RP, Mencherini T, Loggia RD, Tubara A (2007) Characterization of topical antiinflammatory compounds in *Rosmarinus officinalis* L. *J Agric Food Chem* 55: 1718–1723.
- Balasubramanian R, Sughir AA, Damodar G (2012) Oleogel: A promising base for transdermal formulations. *Asian J Pharm* 6: 1–9.
- Bombor R, Horsch W (1977) Properties and evaluation of oleogels. Preparation technology and stability from a rheological standpoint. *Pharmazie* 32: 706–708.
- Brunauer S, Emmett P, Teller E (1938) Adsorption of gases in multimolecular layers. *J Am Chem Soc* 60: 309–319.
- Dassanayake LSK, Kodali DR, Ueno S (2011) Formation of oleogels based on edible lipid materials. *Curr Opin in Colloid and Interface Sci* 16: 432–439.
- Ekman R (1983) The Submarin monomers and triterpenoids from the outer bark of *Betula verrucosa* Ehrh. *Holzforschung* 37: 205–211.
- Geisseler G, Seidel H (1977) Die Wasserstoffbrückenbindung. Vieweg u. Sohn, Braunschweig, und Akademie-Verlag, Berlin.
- Günzler H, Gremlich H-U (2003) IR-Spektroskopie. WILEY-VCH Verlag GmbH & Co. KGaA, Weinheim.
- Henrich B, Wonisch A, Kraft T, Moseler M, Riedel H (2007) Simulations of the influence of rearrangement during sintering. *Acta Materialia* 55: 753–762.
- Jäger S, Winkler K, Pfüller U, Scheffler A (2007) Solubility studies of oleanolic acid and betulinic acid in aqueous solutions and plant extracts of *Viscum album* L. *Planta Med* 73: 157–162.
- Jäger S, Laszczyk MN, Scheffler A (2008) A preliminary pharmacokinetic study of betulin, the main pentacyclic triterpene from extract of outer bark of birch (*Betulae alba cortex*). *Molecules* 13: 3224–3235.
- Kutz G, Daniels R, Trommer H (2011) Emulsionen. Verlag für Medizin und Naturwissenschaften GmbH, Aulendorf.
- Laredo T, Barbut S, Marangoni AG (2011) Molecular interactions of polymer oleogelation. *Soft Matter* 7: 2734–2743.
- Laszczyk M, Jäger S, Simon-Haarhus B, Scheffler A, Schempp CM (2006) Physical, chemical and pharmacological characterization of a new oleogel-forming triterpene extract from the outer bark of birch (*Betulae Cortex*). *Planta Med* 72: 1389–1395.
- Laszczyk M (2007) Triterpentrockenextrakt aus Birkenkork (*Betula alba cortex*); Untersuchungen zur chemischen Zusammensetzung, Galenik, Penetration und pharmakologisch-biologischen Wirkung. Thesis: Albert-Ludwigs-Universität Freiburg.
- Laszczyk MN (2009) Pentacyclic triterpenes of the lupane, oleanane and ursane group as tools in cancer therapy. *Planta Med* 75: 1549–1560.
- Moura-Letts G (2006) *In vivo* wound-healing activity of oleanolic acid derived from the acid hydrolysis of *Anredera diffusa*. *J Nat Prod* 69: 978–979.
- Murdan S (2005) Organogels in drug delivery. *Expert Opin Drug Deliv* 2: 489–505.
- Pavlova NI, Savinova OV, Nikolaeva SN, Boreko EI, Flekhter OB (2003) Antiviral activity of betulin, betulinic and betulonic acids against some enveloped and non-enveloped viruses. *Fitoterapia* 74: 489–492.
- Sánchez R, Franco JM, Delgado MA, Valencia C, Gallegos C (2011) Rheological and mechanical properties of oleogels based on castor oil and cellulotic derivatives potentially applicable as bio-lubricating greases: influence of cellulotic derivatives concentration ratio. *J Ind Engin Chem* 17: 705–711.
- Schatt W (1992) Sintervorgänge. VDI-Verlag, Düsseldorf.
- Tramosljika D (2007) Sinterverhalten einer bei niedrigen Temperaturen sinternenden Keramik und der Einfluss von Silber auf deren Sinterverhalten. Thesis: Universität; Stuttgart.